Pergamon

Cement and Concrete Research 33 (2003) 223–232

CEMENT AND CONCRETE RESEARCH

Autogenous shrinkage in high-performance cement paste: An evaluation of basic mechanisms

Pietro Lura[a,*], Ole Mejlhede Jensen[b], Klaas van Breugel[a]

[a]*Concrete Structures Group, Faculty of Civil Engineering and Geosciences, Delft University of Technology, P.O. Box 5048, 2600 GA Delft, The Netherlands*
[b]*Department of Building Technology and Structural Engineering, Aalborg University, Sohngaardsholmsvej 57, 9000 Aalborg, Denmark*

Received 7 February 2002; accepted 28 April 2002

Abstract

In this paper, various mechanisms suggested to cause autogenous shrinkage are presented. The mechanisms are evaluated from the point of view of their soundness and applicability to quantitative modeling of autogenous shrinkage. The capillary tension approach is advantageous, because it has a sound mechanical and thermodynamical basis. Furthermore, this mechanism is easily applicable in a numerical model when dealing with a continuously changing microstructure. In order to test the numerical model, autogenous deformation and internal relative humidity (RH) of a Portland cement paste were measured during the first week of hardening. The isothermal heat evolution was also recorded to monitor the progress of hydration and the elastic modulus in compression was measured. RH change, degree of hydration and elastic modulus were used as input data for the calculation of autogenous deformation based on the capillary tension approach. Because a part of the RH drop in the cement paste is due to dissolved salts in the pore solution, a method is suggested to separate this effect from self-desiccation and to calculate the actual stress in the pore fluid associated with menisci formation.

Keywords: Humidity; Shrinkage; Cement paste; Modeling; Self-desiccation

1. Introduction

In high-performance concrete, the low water/binder ratio and the addition of silica fume cause a significant drop in the internal relative humidity (RH) in the cement paste during sealed hydration [1]. Closely related to this autogenous RH change, the cement paste undergoes autogenous shrinkage. In concrete, autogenous shrinkage results in tensile stresses in the cement paste due to restraint from the aggregates [2]. Autogenous shrinkage should be limited because it may induce microcracking or macrocracking and impair the concrete quality [3].

Autogenous shrinkage of concrete is a phenomenon known from the beginning of the 20th century, but its practical importance has only been recognized in recent years. Despite the growing interest in autogenous deformation, no consensus has yet been reached in the scientific community on standard test methods and on the terminology, although some attempts have been made in this direction [4]. In the following, the terminology proposed by Jensen and Hansen [5] will be adopted.

The mechanisms leading to autogenous shrinkage are poorly understood. While there is general agreement about the existence of a relationship between autogenous shrinkage and RH changes in the pores of the hardening cement paste, the actual mechanisms are unknown. Changes in the surface tension of the solid gel particles, disjoining pressure and tension in capillary water are the principal factors that have been debated. For each of these approaches, knowledge of the development of the pore volume and pore size distribution, of the state of water in the capillary pores (free or adsorbed) and of the stiffness of the solid skeleton as hydration proceeds is needed.

2. Modeling autogenous shrinkage—driving forces

2.1. Chemical shrinkage and self-desiccation

Hydration of Portland cement is accompanied by a chemical shrinkage. The chemical shrinkage amounts typ-

* Corresponding author. Tel.: +31-152784580; fax: +31-152785895.
E-mail address: p.lura@citg.tudelft.nl (P. Lura).

0008-8846/02/$ – see front matter © 2002 Elsevier Science Ltd. All rights reserved.
PII: S0008-8846(02)00890-6

ically to 6–7 ml/100 g of cement reacted [6]. Not only hydration of the main clinker minerals but also the secondary reactions, including formation of ettringite, result in chemical shrinkage [7]. Even greater shrinkage is found in the reaction of silica fume with calcium hydroxide: about 20 ml/100 g of silica fume reacted [8].

As long as the cement paste is fluid, the chemical shrinkage is totally converted into an external volume change. In other words, the fluid paste is not able to sustain the internal voids created by chemical shrinkage and contracts. When the hydrates percolate and the first solid paths are formed in the hardening paste, the stiffness increases and gas bubbles start to nucleate and grow in the bigger pores (Fig. 1). This gives rise to the formation of water–air menisci and the RH drops (Kelvin's law). The presence of menisci causes tensile stresses in the pore fluid (Laplace's law). The RH drop results in a change in the thickness of the water layer adsorbed on the solid surfaces [9]. This is accompanied by changes both in the surface tension of the solids and in the disjoining pressure of adsorbed water between solid surfaces. At this early stage of hydration, the stiffness of the paste is so low and the viscous behavior so pronounced that the slightest stress acting on the system results in a large deformation.

2.2. Surface tension

According to the surface tension approach, bulk shrinkage and expansion of the cement paste are results of changes in the surface tension of the cement gel particles. Adsorption of water lowers the surface tension of the cement gel particles and results in expansion. Conversely, removal of adsorbed water causes shrinkage.

Bangham and Fakhoury [10] proposed an equation that relates swelling of coal to changes in the surface tension via a proportionality constant. According to Hiller [11], the constant depends only on the internal surface of the porous body, on the density of the solid and on the elastic modulus of the porous material. Wittmann [12] used a similar relationship to model the swelling of a hardened cement paste and Koenders [13] to model autogenous shrinkage of a hardening cement paste.

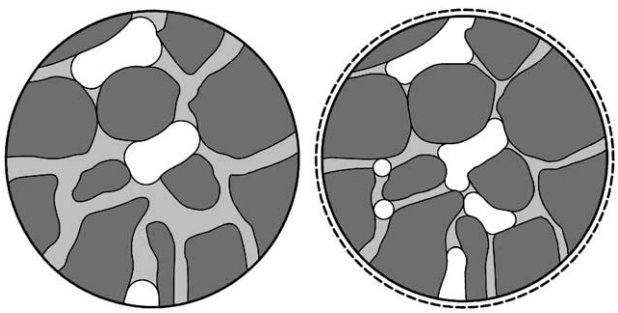

Fig. 1. Schematic representation of a cross-section of hydrating cement paste. Left: low degree of hydration. Right: high degree of hydration. Solid matter (hydrates and unhydrated cement) is shown as dark gray, pore water as light gray and empty pore volume as white. The figure illustrates the formation of empty pore volume due to chemical shrinkage, which results in a decrease of the radius of curvature of the menisci and in bulk shrinkage due to increased tensile stresses in the pore water, i.e., self-desiccation shrinkage (from Ref. [5]).

However, according to Wittmann [14], this linear relationship between deformation and changes in the surface tension must be considered as semiphenomenological. The surface tension mechanism can account only for a small part of the total shrinkage, because it acts on the solids alone and only indirectly on the whole porous body [15]. Moreover, the changes in the surface tension of the solids due to adsorption of water molecules are of significance for the first three adsorbed layers only. The outer layers are bound by weak forces and their influence on the surface tension of the adsorbent is almost negligible. Therefore, the relative importance of the surface tension is higher the lower the RH. This mechanism may not play a major role in autogenous deformation, where normally the RH does not drop under 75% [16].

2.3. Disjoining pressure

The disjoining pressure is active in areas of hindered adsorption, i.e., where the distances between the solid surfaces are smaller than two times the thickness of the free adsorbed water layer. This effect should be of major importance at high RH, because the change in the number of adsorbed water layers is very steep in this region [9]. The disjoining pressure between the solid particles is the result of van der Waals forces, double layer repulsion and structural forces [17]. The disjoining pressure varies with the RH and with the concentration of Ca^{2+} ions in the pore fluid [18]. When the RH drops, the disjoining pressure is reduced [17,18], causing shrinkage.

Nielsen [19] proposed a relationship between RH changes and disjoining pressure in hardened cement pastes. In order to quantify the effect of the change of disjoining pressure on the deformation of the cement paste, its influence area as a function of RH should be known. To this end, Nielsen proposed to determine the pore size distribution of the hardened cement paste through water vapor sorption isotherms. The extension of this approach to hardening cement paste is extremely difficult. A first problem is the rapid change in the properties of the cement paste due to the progress of hydration. A second problem is the very weak structure of the cement paste that might be damaged by drying.

2.4. Capillary tension

The capillary tension in the pore fluid is related to the water–air menisci in the partly empty pores. Its effect should be present in the upper RH range, above about 45% RH [20]. Hua et al. [21] applied this approach to calculate autogenous shrinkage of cement paste. Experimentally, they used mercury intrusion porosimetry (MIP) to

indirectly determine the capillary tension of the pore water. Some difficulties are connected with this technique. For example, the drying of the paste before the MIP measurements take place may modify the pore structure, especially in the first days of hydration. Also, big internal pores that are accessible only through small entries are identified as smaller ones—the so-called inkbottle effect [22]. A more direct approach is to calculate the capillary depression from an internal state parameter of the hardening cement paste, such as the internal RH. Jensen [7] calculated the slope of the autogenous shrinkage a few days after casting with the capillary tension approach using RH measurements to calculate the capillary depression. A good agreement with experimental results was obtained.

An advantage of the capillary tension approach compared with the other mechanisms discussed above is that, once the capillary tension of the pore water is calculated, one only needs to know the degree of saturation and the deformability of the paste to estimate the autogenous deformation [23]. Thus, no information on the internal surface area or on the pore size distribution of the hardening cement paste is needed.

3. Materials and methods

Autogenous deformations, RH change, isothermal heat evolution and elastic modulus of a Portland cement paste were measured during the first week of hardening. The results were used to verify the numerical model for the calculation of autogenous shrinkage.

3.1. Materials

In the present study, Portland cement (CEM I 52.5 R) was used. The calculated Bogue composition of the Portland cement (mass fractions) was C_3S 53.6%, C_2S 20.1%, C_3A 8.2% and C_4AF 9.1%. The composition measured by the producer (ENCI) with XRD was C_3S 63%, C_2S 13%, C_3A 8% and C_4AF 9%.

The *w*/*c* ratio of the paste was 0.37. Silica fume with a BET surface area of 19 m^2/g was added in slurry form, 5.2% by cement mass. A lignosulfonate-based plasticizer (0.2%) and a naphthalene-sulfonate-based superplasticizer (1.7%) were also added to the mix. Then, 1.5 l of cement paste were mixed in a 5 l epicyclic Hobart mixer. Demineralized water was previously mixed with the admixtures and added in two steps to ensure homogeneity. Total mixing time from first water addition was 5 min.

3.2. Autogenous RH measurements

The fresh paste was cast into the measuring chamber of two Rotronic hygroscopic DT stations equipped with WA-14TH and WA-40TH measuring cells. The RH stations were placed in a thermostatically controlled room at 20 ± 0.1 °C. The development of the RH in the samples and the temperature were continuously measured for a period of about 1 week after mixing. Before and after the measurements, calibration of the stations was carried out with four saturated salt solutions in the range of 75–100% RH. This procedure results into a measuring accuracy of about ±1% RH.

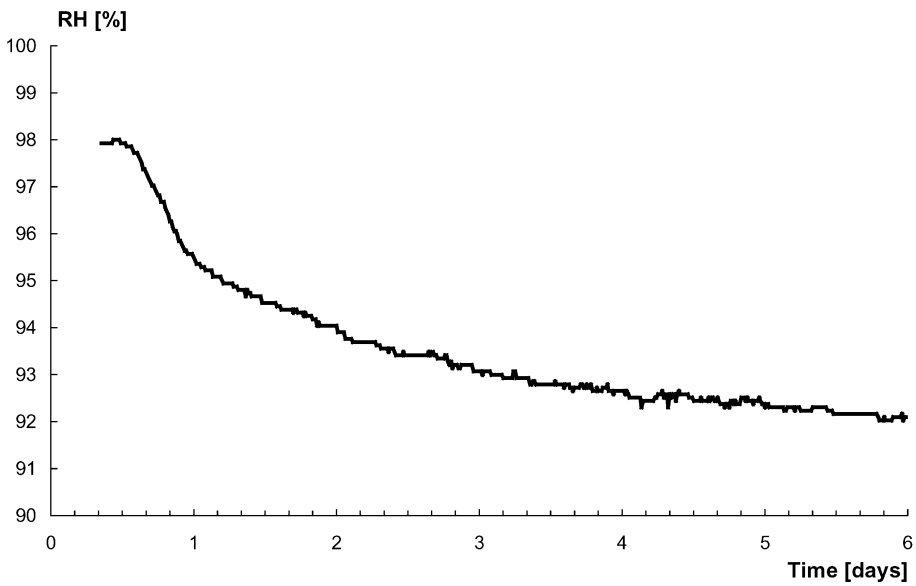

Fig. 2. Autogenous internal RH measured on cement paste. Temperature 20 ± 0.1 °C. Average of two samples.

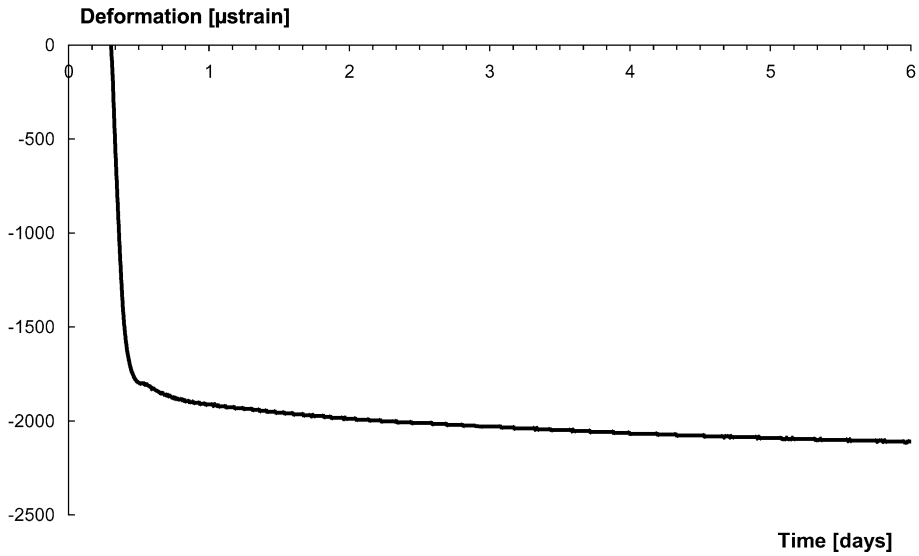

Fig. 3. Autogenous deformation measured on cement paste after setting. Temperature 20 ± 0.1 °C. Average of two samples.

3.3. Autogenous deformation measurements

The cement paste was cast under vibration into tight plastic moulds, which were corrugated to minimize restraint on the paste. The length of the samples was approximately 300 mm. The specimens were placed in a dilatometer, which was immersed into a temperature-controlled glycol bath at 20 ± 0.1 °C. Two samples were tested simultaneously in the dilatometer, with a measuring accuracy of ± 5 microstrain. Continuous linear measurements were started directly after casting. A detailed description of the dilatometer can be found in Ref. [24].

3.4. Isothermal heat evolution

The rate of heat evolution of the cement paste was measured with isothermal calorimetry at 20 °C (3114/3236 TAM Air Isothermal Calorimeter by Thermometric AB).

3.5. Elastic modulus

The elastic modulus in compression was tested on sealed cement paste prisms (50 × 50 × 200 mm) at 1, 3 and 7 days of hardening. The curing temperature was 20 °C.

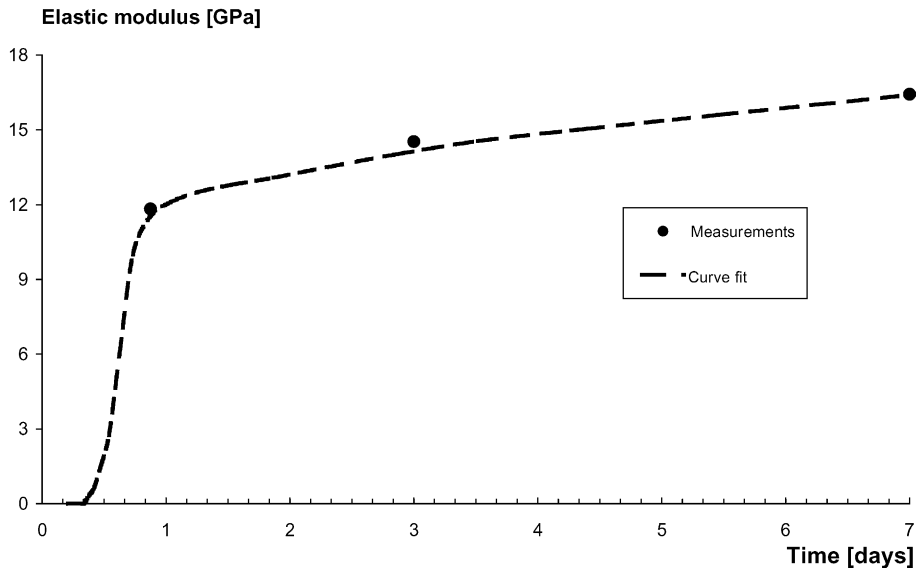

Fig. 4. Measured elastic modulus of cement paste and fitted curve. Curing temperature 20 °C. Average of two samples.

4. Results

Autogenous RH is shown in Fig. 2 and autogenous deformation is shown in Fig. 3. In Fig. 3, the deformations were zeroed at the time of setting, about 8 h after mixing with water. A significant change in the slope of the deformations occurred at about 12 h, when the shrinkage was 1750 microstrain. This point corresponds to the moment when the RH started to drop (see Fig. 2).

The measured elastic modulus is shown in Fig. 4 together with an interpolated curve.

5. Discussion

5.1. Autogenous RH change

The measured RH drop (Fig. 2) from approximately 12 h and onwards occurs in the set cement paste. Consequently, it is attributed to self-desiccation of the cement paste. However, the RH was about 98% before setting, when the cement is fluid and the pore system is saturated. This initial RH drop can be attributed to dissolved salts in the pore fluid [25]. The RH due to dissolved salts in the pore fluid can be estimated with Raoult's law (Eq. (1)) [25]:

$$\mathrm{RH}_S = X_1 \tag{1}$$

where X_1 is molar fraction of water in the pore fluid.

Based on expressed pore fluid compositions and Raoult's law, the RH drop due to dissolved salts may amount to several percent. For example, for a composition of the pore fluid reported by Page and Vennesland [26] for a 2-month-old cement paste with $w/c = 0.45$, a value of 96.7% RH is found. This 3.3% RH drop is mainly due to the alkali hydroxides and not to the Ca^{2+} ions, whose solubility is depressed by the presence of the former.

As a consequence of hydration, the cement paste forms a solid skeleton. From the formation of the solid skeleton, the chemical shrinkage is not totally transformed into external volume change. If the water supply is restricted, empty pores are formed inside the paste and air–water menisci occur. The air bubbles in the cement paste are formed in the bigger pores (Fig. 1), which consequently empty first. Simultaneously, a drop in the RH occurs. The RH due to meniscus formation in a circular cylindrical pore can be calculated according to Kelvin's equation:

$$\mathrm{RH}_K = \exp\left(-\frac{2\gamma M\cos\theta}{\rho r RT}\right) \tag{2}$$

where γ is surface tension of water (0.073 N/m in pure water), M is molar weight of water (0.01802 kg/mol), θ is contact angle between water and solids, ρ is density of water (approximately 1000 kg/m^3), r is radius of the meniscus, R is ideal gas constant (8.314 J/mol K) and T is absolute temperature (in this paper, 293.15 K).

Assuming perfect wetting, the contact angle between water and solids is zero. Thus, $\cos\theta = 1$. For θ close to 0, $\cos\theta \cong 1$. With this assumption, the radius of the largest capillary pore filled with water can be calculated by rearranging Eq. (2):

$$r = -\frac{2\gamma M}{\ln(\mathrm{RH}_K)\rho RT} \tag{3}$$

If we take into account the RH drop both due to menisci formation and due to dissolution of salts, the total RH can be approximated according to the following formula [25]:

$$\mathrm{RH} = \mathrm{RH}_S\mathrm{RH}_K = X_1\exp\left(-\frac{2\gamma M}{\rho r RT}\right) \tag{4}$$

Note that the presence of the dissolved salts influences the total RH also indirectly through RH_K, because dissolved salts lower the surface tension γ. For a pore fluid, about 0.055 N/m was measured with a du Noüy tensiometer [7].

To calculate the radius of the largest capillary pore filled with water directly from the RH measurements, the influence of the dissolved salts has also to be taken into consideration by combination of Eqs. (3) and (4):

$$r = -\frac{2\gamma M}{\ln\left(\frac{\mathrm{RH}}{\mathrm{RH}_S}\right)\rho RT} \tag{5}$$

Assuming that the RH drop measured in the first hours (about 2%) is due only to dissolved salts and further that this effect remains constant during hydration, it is possible to calculate the RH drop due to menisci formation for the cement paste studied. Measured and calculated RH values are shown in Fig. 5.

5.2. Kelvin radius and tensile stress in the pore fluid

Once the RH drop due to self-desiccation is separated from the one due to salt dissolution, it is possible to calculate the actual Kelvin radius from the measured RH with Eq. (5). Results are shown in Fig. 6. The thin line shows the Kelvin radius calculated with Eq. (3), assuming a surface tension of 0.055 N/m for the pore fluid [7]. It is noticed that, at 98% RH, Eq. (3) predicts that all the pores with a radius over 0.04 μm are empty. This can obviously not be the case, because the cement paste, before setting, is still semifluid and saturated. On the other hand, according to Eq. (5) (bold line in Fig. 6), at 98% RH, all the pores are water filled. As the RH drops, differences between the two curves presented in Fig. 6 diminish.

When the Kelvin radius is known, the tensile stress in the pore fluid can be calculated with the Laplace law for circular cylindrical pores:

$$\sigma_{\mathrm{cap}} = \frac{2\gamma}{r} \tag{6}$$

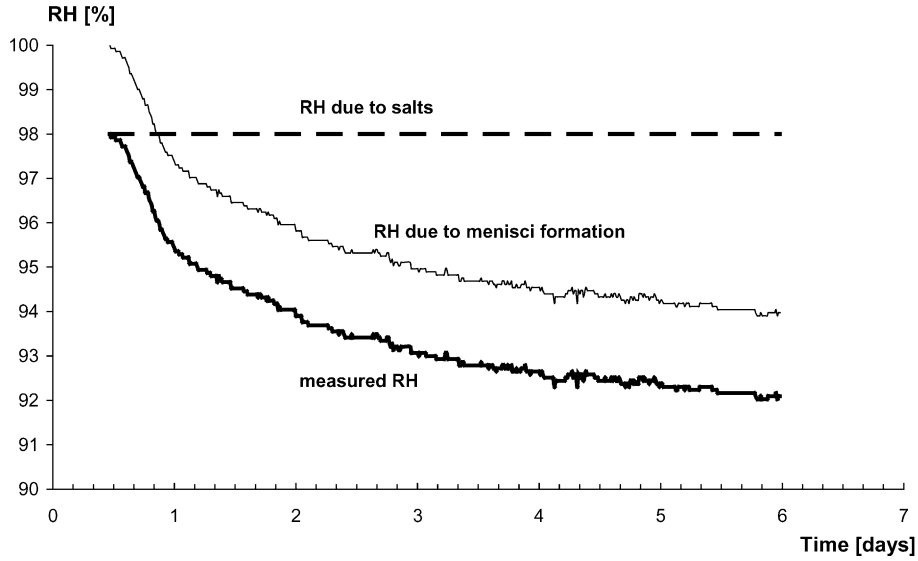

Fig. 5. Autogenous RH in a cement paste during sealed hardening separated with Eq. (4) according to different contributions.

5.3. Deformation of the cement paste

The deformation of the cement paste is calculated according to the following equation [23]:

$$\varepsilon_{LIN} = \frac{S\sigma_{cap}}{3}\left(\frac{1}{K} - \frac{1}{K_S}\right) \tag{7}$$

where S is saturation fraction (−), σ_{cap} is stress in the pore fluid (MPa), K is bulk modulus of the whole porous body (MPa) and K_S is bulk modulus of the solid material (MPa). Strictly speaking, this equation is only valid for a fully saturated linear elastic material. It is only approximate at partial saturation and creep is not taken into account.

The saturation fraction can be calculated as the ratio between the evaporable water content in the sealed hardening paste (V_{ew}) and the total pore volume of the paste (V_p), which are both functions of the w/c ratio and of the degree of hydration α:

$$S = \frac{V_{ew}(\alpha)}{V_p(\alpha)} \tag{8}$$

5.3.1. Powers' volumetric model for Portland cement paste

If we consider a Portland cement paste and apply Powers' model (see Appendix A) to calculate the non-

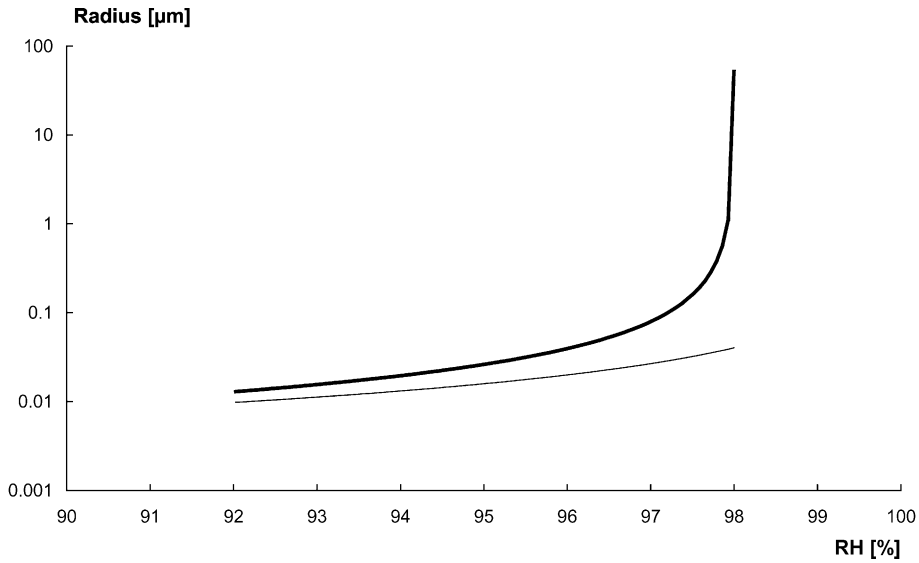

Fig. 6. Kelvin's radius calculated with (bold line) and without (thin line) correction for the influence of dissolved salts. The RH drop due to salts (2%) is assumed constant (see Fig. 5).

evaporable water and the total pore volume, Eq. (8) becomes [8]:

$$S = \frac{V_{ew}(\alpha)}{V_p(\alpha)} = \frac{V_{cw}(\alpha) + V_{gw}(\alpha)}{V_{cw}(\alpha) + V_{gw}(\alpha) + V_{cs}(\alpha)} = \frac{p - 0.7(1-p)\alpha}{p - 0.5(1-p)\alpha} \quad (9)$$

where $V_{cw}(\alpha)$ is capillary water (m^3/m^3), $V_{gw}(\alpha)$ gel water (m^3/m^3) and $V_{cs}(\alpha)$ chemical shrinkage (m^3/m^3)

$$p = \frac{w/c}{(w/c) + (\rho_W/\rho_C)}.$$

The development of the degree of hydration α in time can be estimated by isothermal calorimetry, according to the following formula (Eq. (10)):

$$\alpha = \frac{Q}{Q_{pot}}. \quad (10)$$

In the calculation, special attention has to be given to the value of the potential heat of hydration, Q_{pot}, which is the heat developed at complete hydration. The cement in this study is assumed to have a potential heat of hydration of 535 kJ/kg. Based on isothermal calorimetry (see Section 3.4), Fig. 7 shows the development of the degree of hydration in the paste.

5.3.2. Powers' volumetric model for silica fume-modified cement paste

The cement paste also contains 5.2% silica fume (see Section 3.1). Silica fume modifies substantially the properties of the paste, especially the RH change and the autogenous deformation [1]. To take the presence of silica fume into account, Powers' model modified for silica fume addition was applied (see Appendix A and Ref. [7]):

$$S = \frac{V_{cw}(\alpha) + V_{gw}(\alpha)}{V_{cw}(\alpha) + V_{gw}(\alpha) + V_{cs}(\alpha)} = \frac{p - 0.8k(1-p)\alpha}{p - k(0.6 - 0.7(s/c))(1-p)\alpha} \quad (11)$$

where

$$p = \frac{w/c}{(w/c) + (\rho_W/\rho_C) + (\rho_W/\rho_S)(s/c)}$$

$$k = \frac{1}{1 + 1.4(s/c)}$$

and s/c = silica fume/cement ratio.

In Fig. 7, the development in time of the saturation fraction is shown, calculated both using Powers' model (Eq. (9)) and the model modified for silica fume (Eq. (11)). It is noticed that the saturation fraction changes by the addition of 5% silica fume.

If we multiply the tensile stress in the pore water by the saturation fraction S, the bulk stress acting on the solid skeleton is obtained (Fig. 8). The bulk stress is lower than the capillary stress, as the saturation fraction is always lower than unity. If the model including silica fume is used for the calculation (Eq. (11)), the calculated internal stress is slightly lower.

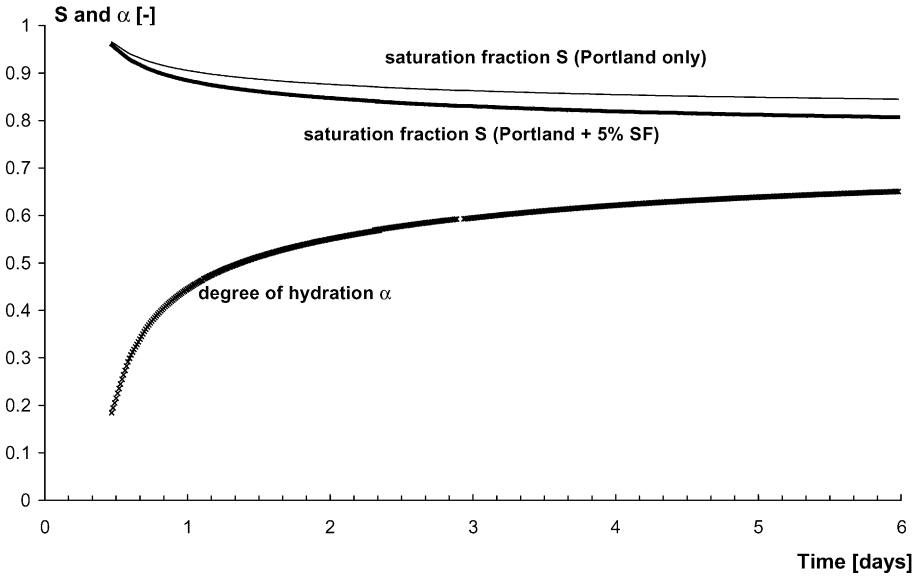

Fig. 7. Measured degree of hydration and calculated saturation fraction of the cement paste during sealed hydration as a function of time.

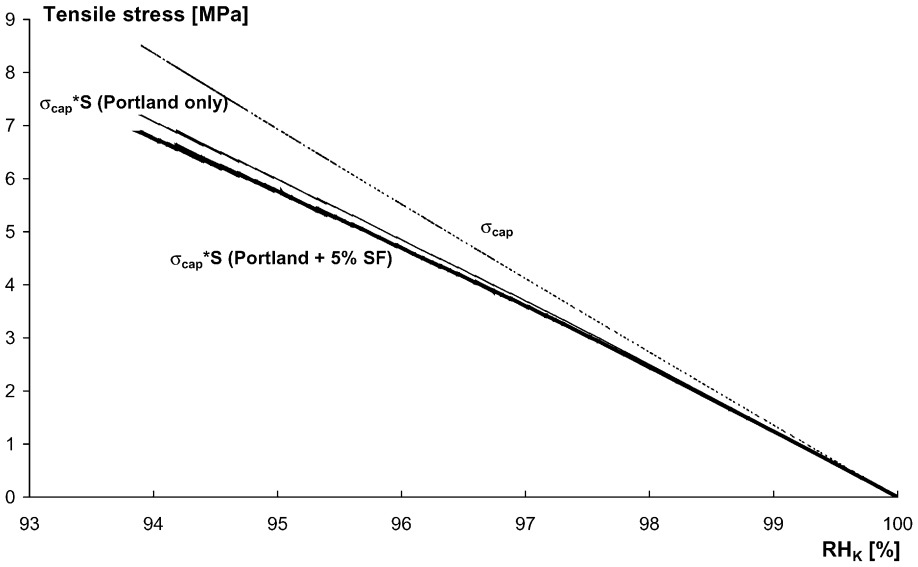

Fig. 8. Stresses in the pore water (σ_{cap}) and bulk stress in the unit volume ($\sigma_{cap}S$) as a function of RH_K.

5.4. Bulk modulus of the cement paste and of the solid material

The bulk modulus K of the cement paste was calculated using the following formula (Eq. (12)):

$$K = \frac{E}{3(1-2\nu)} \tag{12}$$

where E is elastic modulus (MPa) and ν is Poisson's ratio (–).

The measured elastic modulus and the fitted curve are shown in Fig. 5.

The bulk modulus of the solid material ($K_S = 44$ GPa) and the Poisson's ratio ($\nu = 0.2$) were obtained from the literature [19].

5.5. Calculation of autogenous deformation

The autogenous deformation of the cement paste was calculated according to Eq. (7), where S was calculated with Eq. (9) or Eq. (11), σ_{cap} with Eq. (6) and K and K_S as explained in Section 5.4. In Fig. 9, the autogenous deformation is plotted against the RH induced by menisci formation (RH_K). Only the part of the deformation occurring after the start of the RH drop is shown. The calculated values agree very well with the experimental ones down to a RH_K of 97%. Then, the measured deformation increases while the calculated one remains almost constant, which is due both to the flattening out of the bulk stress in the cement paste (Fig. 7) and to the increase of the elastic modulus (Fig. 4).

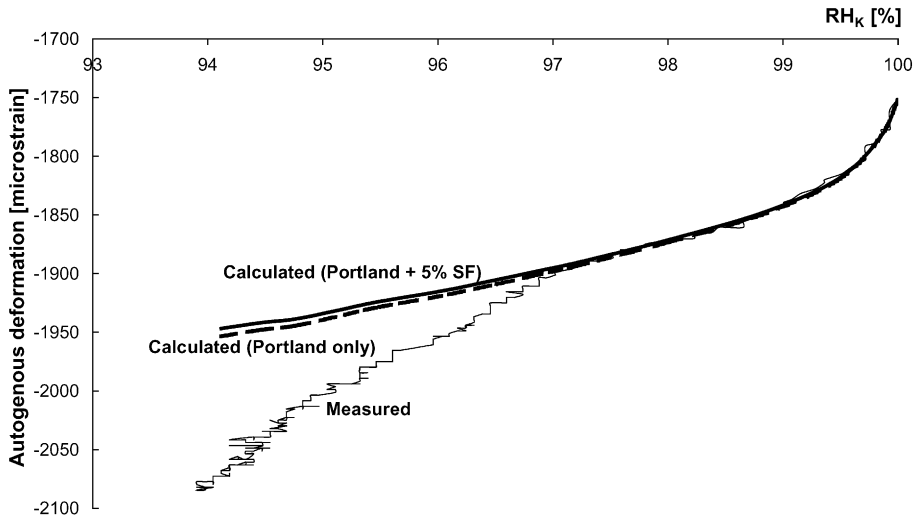

Fig. 9. Measured and calculated autogenous deformation plotted vs. RH due to menisci formation (RH_K).

It must be noticed that Eq. (7) supposes an elastic behavior of the cement paste. In fact, in the first 24 h, the slope of the measured shrinkage decreases, corresponding to an increase of the elastic modulus of the cement paste. Afterwards, the RH drop slows (Fig. 3) and the deformation per percent RH increases. This fact could be due to the onset of the pozzolanic reaction of silica fume that consumes the calcium hydroxide crystals. Internal restraints in the paste (represented by the calcium hydroxide crystals) are removed, inducing additional shrinkage [1]. Another possible reason could be creep of the cement paste. Perhaps the effect of creep becomes evident at lower RH, because in the second part of the curve the deformations occurred during a longer time span.

6. Conclusions

Autogenous shrinkage of a hardening cement paste was calculated with a combined experimental and numerical approach. Isothermal heat evolution, elastic modulus in compression and autogenous RH were measured in the first week after casting. These quantities were used as input for the calculation of autogenous shrinkage based on the capillary tension approach. Because the autogenous RH change is due to dissolved salts in the pore fluid as well as to meniscus formation, a method was developed to separate these two effects. This allowed the calculation of the actual stress in the pore fluid that is associated with menisci formation. The calorimetric data were used to calculate the development of the degree of hydration. With Powers' volumetric model for cement hydration and Powers' volumetric model modified for silica fume addition, the saturation fraction was estimated. The linear autogenous deformation was calculated on the basis of the capillary tension, the saturation fraction and the bulk modulus of the paste. Simulated shrinkage curves were in good agreement with the experiments in the higher RH range, while they underestimated the measured autogenous deformation as the RH further decreased, possibly due to the influence of creep or to the pozzolanic reaction of silica fume.

Appendix A. Powers' volumetric model for cement paste and silica fume-modified cement paste

A.1. Phase composition of hardening Portland cement paste

The following set of formulas describes Powers' model for the phase composition of a hardening Portland cement paste.

Chemical shrinkage: $V_{cs} = 0.2(1-p)\alpha$
Capillary water: $V_{cw} = p - 1.3(1-p)\alpha$
Gel water: $V_{gw} = 0.6(1-p)\alpha$
Gel solid: $V_{gs} = 1.5(1-p)\alpha$
Cement: $V_c = (1-p)(1-\alpha)$

where

$$\sum_i V_i = 1$$

and

$$p = \frac{w/c}{(w/c) + (\rho_W/\rho_C)}$$

w and c refer to masses of water and cement, respectively, with $\rho_C \cong 3150$ kg/m^3 and $\rho_W \cong 1000$ kg/m^3.

The constants in Powers' volumetric model are derived from the following data:

Nonevaporable water: $W_n = 0.23$ g/g cement reacted
Gel water: $W_{gw} = 0.19$ g/g cement reacted
Chemical shrinkage: $\Delta V = 6.4$ ml/100 g cement reacted

A.2. Phase composition of hardening Portland cement paste with silica fume addition

The following set of formulas describes Powers' volumetric model for the phase composition of a hardening Portland cement paste with silica fume addition. N.B.: In the formulas, it is assumed that the silica fume reacts proportionally to the cement.

Chemical shrinkage: $V_{cs} = k(0.2 + 0.7(s/c))(1-p)\alpha$
Capillary water: $V_{cw} = p - k(1.4 + 1.6(s/c))(1-p)\alpha$
Gel water: $V_{gw} = k(0.6 + 1.6(s/c))(1-p)\alpha$
Gel solid: $V_{gs} = k(1.6 + 0.7(s/c))(1-p)\alpha$
Cement: $V_c = k(1-p)(1-\alpha)$
Silica fume: $V_s = k(1.4(s/c))(1-p)(1-\alpha)$

where

$$\sum_i V_i = 1$$

$$p = \frac{w/c}{(w/c) + (\rho_W/\rho_C) + (\rho_W/\rho_S)(s/c)}$$

$$k = \frac{1}{1 + 1.4(s/c)}$$

w, c and s refer to masses of water, cement and silica fume, respectively, with $\rho_C \cong 3150$ kg/m^3, $\rho_S \cong 2200$ kg/m^3 and $\rho_W \cong 1000$ kg/m^3.

The constants in the model are derived from the data shown in Section A of Appendix A, with the addition of similar data for the silica fume pozzolanic reaction:

Nonevaporable water: $W_n = 0$ g/g silica fume reacted
Gel water: $W_{gw} = 0.5$ g/g silica fume reacted
Chemical shrinkage: $\Delta V = 20$ ml/100 g silica fume reacted

References

[1] O.M. Jensen, P.F. Hansen, Autogenous deformation and change of the relative humidity in silica fume-modified cement paste, ACI Mater. J. 93 (6) (1996) 539–543.

[2] B.F. Dela, Eigenstresses in hardening concrete, PhD thesis, Department of Structural Engineering and Materials, The Technical University of Denmark, Lyngby, Denmark, 2000.

[3] A.M. Paillere, M. Buil, J.J. Serrano, Effect of fiber addition on the autogenous shrinkage of silica fume concrete, ACI Mater. J. 86 (2) (1989) 139–144.

[4] Technical Committee on Autogenous Shrinkage of Concrete, Japan Concrete Institute, Japan Concrete Institute Committee report, in: E.-I. Tazawa (Ed.), Autogenous Shrinkage of Concrete, Proc. Int. Workshop AUTOSHRINK'98, Hiroshima, 13–14 June 1998, E&FN Spon, London, 1999, pp. 1–67.

[5] O.M. Jensen, P.F. Hansen, Autogenous deformation and RH-change in perspective, Cem. Concr. Res. 31 (12) (2001) 1859–1865.

[6] T.C. Powers, T.L. Brownyard, Studies of the physical properties of hardened Portland cement paste (nine parts), J. Am. Concr. Inst. 43 (Oct. 1946–April 1947), Bulletin 22, Research Laboratories of the Portland Cement Association, Chicago, 1948.

[7] O.M. Jensen, Autogenous deformation and RH-change—self-desiccation and self-desiccation shrinkage. Appendix-measurements and notes (in Danish), Building Materials Laboratory, The Technical University of Denmark, Lyngby, Denmark, 1993, TR 285/93.

[8] O.M. Jensen, P.F. Hansen, Water-entrained cement-based materials: I. Principles and theoretical background, Cem. Concr. Res. 31 (5) (2001) 647–654.

[9] J. Hagymassy, J.R. Brunauer, R.S. Mikhail, Pore structure analysis by water vapor adsorption, J. Colloid Interface Sci. 29 (3) (1969) 485–491.

[10] D.H. Bangham, N. Fakhoury, The swelling of charcoal, Proc. R. Soc. Lond. (1931) 81–89.

[11] K.H. Hiller, Strength reduction and length changes in porous glasses caused by water vapour adsorption, J. Appl. Phys. 35 (1964) 1622–1628.

[12] F.H. Wittmann, Grundlagen eines Modells zur Beschreibung charakteristischer Eigenschaften des Betons, Dtsch. Aussch. Stahlbeton 290 (1977) 42–101.

[13] E.A.B. Koenders, Simulation of volume changes in hardening cement-based materials, Delft University of Technology, PhD thesis, Delft, The Netherlands, 1997.

[14] F.H. Wittmann, The structure of hardened cement paste—A basis for a better understanding of the material properties, Proc. Conf. on Hydraulic Cement Pastes: Their Structure and Properties, Sheffield, Cement and Concrete Association, Slough, 1976, pp. 96–117.

[15] T.C. Powers, Mechanisms of shrinkage and reversible creep of hardening cement paste, Proc. Int. Symp. Structure of Concrete and its Behaviour Under Load, Cement and Concrete Association, London, 1965, pp. 319–344.

[16] O.M. Jensen, Thermodynamic limitation of self-desiccation, Cem. Concr. Res. 25 (1) (1995) 157–164.

[17] C. Ferraris, F.H. Wittmann, Shrinkage mechanisms of hardened cement paste, Cem. Concr. Res. 17 (1987) 453–464.

[18] F. Beltzung, F.H. Wittmann, L. Holzer, Influence of composition of pore solution on drying shrinkage, in: F.-J. Ulm, Z.P. Bažant, F.H. Wittmann (Eds.), Creep, Shrinkage and Durability Mechanics of Concrete and Other Quasi-Brittle Materials, Proceedings of Sixth International Conference, CONCREEP-6@MIT, Cambridge (MA), USA, Elsevier, Amsterdam, 2001, pp. 39–48.

[19] L.F. Nielsen, A research note on sorption, pore size distribution, and shrinkage of porous materials, Building Materials Laboratory, The Technical University of Denmark, Lyngby, Denmark, 1991, TR 245/91.

[20] I. Soroka, Portland cement paste and concrete, Macmillan, London, 1979.

[21] C. Hua, P. Acker, A. Erlacher, Analyses and models of the autogenous shrinkage of hardening cement paste: I. Modelling at macroscopic scale, Cem. Concr. Res. 25 (7) (1995) 1457–1468.

[22] S. Diamond, Mercury porosimetry—An inappropriate method for the measurement of pore size distributions in cement-based materials, Cem. Concr. Res. 30 (10) (2000) 1517–1525.

[23] D. Bentz, E.J. Garboczi, D.A. Quenard, Modelling drying shrinkage in reconstructed porous materials: Application to porous Vycor glass, Model. Simul. Mater. Sci. Eng. 6 (1998) 211–236.

[24] O.M. Jensen, P.F. Hansen, A dilatometer for measuring autogenous deformation in hardening cement paste, Mater. Struct. 28 (181) (1995) 406–409.

[25] O.M. Jensen, Autogenous deformation and RH-change—self-desiccation and self-desiccation shrinkage (in Danish), PhD thesis, Building Materials Laboratory, The Technical University of Denmark, Lyngby, Denmark, 1993, TR 284/93.

[26] C.L. Page, Ø. Vennesland, Pore solution composition and chloride binding capacity of silica-fume cement pastes, Mater. Struct. 16 (91) (1983) 19–25.